Marked seasonal succession and 'boom-bust' bloom dynamics of diatoms in the sub-tropical Gulf of Aqaba in the Northern Red Sea

Yoav Avrahami

1. Department of Ecology, Evolution and Behavior, Silberman Institute of Life Sciences, The Hebrew University of Jerusalem, Jerusalem, 91904, Israel

2. The Interuniversity Institute for Marine Sciences in Eilat, POB 469, 88103, Eilat, Israel

Gil Koplovitz

The Interuniversity Institute for Marine Sciences in Eilat, POB 469, 88103, Eilat, Israel

Miguel J. Frada[2]

1. Department of Ecology, Evolution and Behavior, Silberman Institute of Life Sciences, The Hebrew University of Jerusalem, Jerusalem, 91904, Israel

2. The Interuniversity Institute for Marine Sciences in Eilat, POB 469, 88103, Eilat, Israel

E-mail: miguel.frada@mail.huji.ac.il

Tel: +972-086360147

Running title: Diatom succession in subtropical ecosystem

Abstract

Diatoms dominate primary production in nutrient-rich ecosystems. Less is known about the diversity and ecology of diatoms in low latitude, oligotrophic ecosystems. Here, we examined using scanning electron microscopy the seasonal succession of planktonic diatoms in the Gulf of Aqaba (Red Sea), a subtropical ecosystem that alternates between stratified, oligotrophic conditions during spring/summer resembling open-ocean oligotrophic regions and deeply mixed, mesotrophic conditions during fall/winter. Diatom diversity and density were both lower during the stratified season. Pennate species comprised >90% of the diatom counts. A shift in diatom density involving an increase in centric diatom dominance was detected at mid-winter, as temperature declined and nitrogen concentrations exceeded ~0.5 µmol L^{-1}. This occurred markedly later relative to total phytoplankton, suggesting higher nutrient requirements for diatom growth. Faster community succession was detected during winter. Peak diatom densities occurred during the mixing-to-stratification transition at the peak of nutrient concentrations, coinciding with the annual peak in chlorophyll a (bloom). Blooms were numerically dominated by small cells, but significant proportions of chain-forming centrics (*Chaetoceros* and *Leptocylindrus*) and spores were also detected specially during colder years as mixing was deeper and nutrient higher. Blooms last about 1-month and declined rapidly to low cell densities, along with water column restratification and nutrient depletion, involving the replacement of centric species by pennates. Overall, marked seasonal dynamics and contrasts were detected, along with distinct variations in the prevalence of pennate, centric and large chain-forming species, highlighting underlying eco-physiological differentiation and the importance of each morpho-group in oligotrophic regimes.

Introduction

Marine phytoplankton form the base of the marine food-web and drive nearly one half of the global primary production (Field et al., 1998). Diatoms (Bacillariophyta) are one of the most prolific phytoplankton groups, responsible for about 40% of the marine primary productivity and acting as a key driver of the biological pump (Falkowski et al., 1998). Given that their composite cell wall is primarily composed of silica, they also play a primary role in the global silica cycle (Falciatore & Bowler, 2002; Tréguer et al., 1995). Two main morphological groups of diatoms exist based on the shape of their main cell wall elements; the valves: centric (valves with radial pattern center from which ribs radiate) and pennate diatoms (valves with keel-like pattern center from which ribs orient perpendicularly) (Round, 1981; Round et al., 1990). Diatom cell-size ranges from a few micrometers up to a few millimeters, where several species form large chains of cells (Fryxell, 1978). Several mechanisms have been suggested to explain the ecological success of diatoms in the contemporary oceans. These include their protective silica encasement against predation (Friedrichs et al., 2013; Hamm et al., 2003), and advantageous adaptations for carbon fixation (López-Sandoval et al., 2014; Riebesell, 2000), high nutrient uptake rates (Rogato et al., 2015), and the ability to form spores, a resting life-stage to survive through detrimental conditions, including nutrient limitation and temperature fluctuations (Davis et al., 1980; Kuwata et al., 1993; Oku & Kamatani, 1995) and viral infections (Pelusi et al., 2021). Diatoms are a cosmopolitan group across the oceans (Malviya et al., 2016). However, they principally prevail in well-mixed coastal and upwelling ecosystems where they effectively exploit intermittent high nutrient loads and turbulent water conditions to sustain high growth rates and henceforth can form extensive blooms (Crawford, 1995; Ruggiero et al., 2018; Sarthou et al., 2005). These blooms form the base of the most important fisheries worldwide (Koeve, 2004; Lassiter et al., 2006). As outlined by Leblanc et al. (Leblanc et al., 2018), the

classical view of diatom spring bloom succession in nutrient rich regions involves a first stage following upwelling or strong mixing that is dominated by smaller fast-growing species (namely of the genera *Thalassiosira* and *Skeletonema*), followed by larger chain-forming species (e.g., of the genus *Chaetoceros*). Then, as the water column becomes stratified and nutrients limiting, species adapted to oligotrophic regimes often carrying N_2-fixing symbionts thrive (e.g., of the genera *Rhizosolenia* and *Hemiaulus*). This view is possibly skewed to large size species, because the collection of water samples typically relies on large-mesh size plankton nets (~20-60 um). However, recent studies of diatom blooms report an actual numerical dominance of very small species (< 5 µm; e.g., of the genera *Minidiscus*, *Thalassiosira*, *Fragilariopsis*, *Nitzschia*, and *Nanoneis*), emphasizing their importance during blooms (Buck et al., 2008; Leblanc et al., 2018; Savidge et al., 1995). In oligotrophic regions of the oceans, diatom biomass is generally low as it is the case for phytoplankton assemblages (Nelson et al., 1995; Tréguer et al., 2018), although intermittent diatom blooms with significant contributions to organic matter export and high diatom densities at the deep- or subsurface chlorophyll maxima have been detected in those type of regions (Brzezinski & Nelson, 1995; Karl et al., 2012). By contrast, diatom diversity can be high, often comparable to coastal, eutrophic areas and comprising large chain-forming species typically linked to bloom conditions (Malviya et al., 2016; Setta et al., 2023); although lower diversity in oligotrophic systems was reported as well, (Busseni et al., 2020). Still studies focusing on diatoms inhabiting oligotrophic environments (Hulburt et al., 1960; Hulburt & Rodman, 1963) are far less frequent as compared to eutrophic regions, limiting current understanding diatom ecology and responses to environmental variability in those regions that comprise large sections of the global ocean and are more susceptible to global warming (Polovina et al., 2008). To address this knowledge-gap, we examined with high temporal and taxonomic

resolution the diversity and ecological succession patterns of diatoms in the sub-tropical ecosystem of the Gulf of Aqaba/ Eilat (GoA) located in the northern Red Sea (Fig. 1). The GoA is a warm, narrow basin surrounded by deserts appended to the northern section Red Sea. From an oceanographic standpoint, the GoA is a subtropical system viewed as an oligotrophic ecosystem. However, strong seasonal variations in nutrient loads are detected. In fact, during the warmer spring and summer seasons (April to September) the water column in the GoA is stratified and oligotrophic, macronutrients are limiting and phytoplankton biomass is low (< 1 µmol L^{-1} nitrate, < 0.15 µmol L^{-1} phosphate, > 0.5 µg L^{-1} chlorophyll a, (Israel National Monitoring Program NMP, www.Iui-Eilat.Ac.Il/Research/NMPAbout.Aspx)), resembling open ocean oligotrophic systems in terms of the structure of the water column and phytoplankton communities (Keuter et al., 2021; Lindell & Post, 1995; Zarubin et al., 2017). Under these conditions, cyanobacteria (*Prochlorococcus* and *Synechococcus*) numerically dominate phytoplankton communities (Lindell & Post, 1995). However, by October surface cooling triggers the erosion of the stratified layer. Continuous cooling through winter drives deep convective mixing to a maximum around March. The amplitude of mixing varies largely between years, approximately ranging from about 300m to exceptional depths of >700m during especially cold winters. The depths of mixing vary as an inverse function of atmospheric temperature in winter and is enabled by a prevailing warm and narrow thermocline gradient across the water column in the GoA (Genin et al., 1995; Zarubin et al., 2017). Deep mixing transports ample nutrients to the photic layer, resulting in marked shifts in the composition and phytoplankton biomass (e.g., Al-Najjar et al., 2007; Keuter et al., 2023; Lindell & Post, 1995). Then, at the onset of spring during March/April, mixing is capped by surface warming, prompting re-stratification of the water column. This physical state of the water sets the conditions for the rise of a prominent phytoplankton bloom in the photic layer dominated by uniquely high chlorophyll densities for a subtropical ecosystem

(Zarubin et al., 2017). Large-chain forming diatoms from the genus *Chaetoceros* has been reported to dominate the integrated photoautotrophic biomass during such bloom (Al-Najjar et al., 2007; Kimor & Golandsky, 1977). However, comprehensive quantitative assessment of the diatom diversity, succession patterns, bloom development and decline are still lacking. In this study, analyses of natural samples were undertaken by scanning electron microscopy for detailed taxonomy and enumeration of individual species. Temporal detail was higher during the winter mixing and bloom periods where species succession was faster. Moreover, higher taxonomic detail was devoted to centric diatom species, while most pennate species with less recognizable morphological features were grouped in broad size categories. Our study provides a detailed baseline information of diatoms in the GoA as well as further understanding on the diversity, patterns of succession and responses of diatom communities to environmental variability in open-ocean subtropical ecosystems.

Methods

Study site and sampling

Sampling was undertaken during 2020-2022 in the open sea station A (29°28’N, 34°55’E) where bottom depth is about 700 m and is located about 3 km off-shore the city of Eilat (Israel) in the Gulf of Aqaba. During winter mixing (October-March), samples were collected at 2 m depth twice a month. Between March and April, when winter mixing ceased and before full stratification, samples were collected weekly or twice per week to capture bloom events. In the bloom of 2022 sampling took place daily for 5 consecutive days. At each time point, ~30 L of seawater was sampled using a manual pump installed in a boat and pre-filtered by 500 µm mesh to avoid large zooplankton and transferred into acid washed carboys. In addition, a Sea-Bird SBE 19 CTD (conductivity, temperature, depth, Sea-Bird Scientific) was deployed to obtain physical parameters of the water-column. Mixed layer

depth (MLD) was calculated according to Zarubin et al. (Zarubin et al., 2017), as the depth in which there is a difference of 0.2 °C of potential temperature, compared to 3m depth. During summer stratification, samples were collected at the end of April (April 27th), May, June, and August, with similar procedures both from the surface but also the DCM using 12 L Niskin bottles (General Oceanics) installed on Sea-Bird carousel and coupled with Sea-Bird SBE 19+ CTD (Sea-Bird Scientific). Within ~30 min of collection, the seawater samples were sub-sampled for nutrients, pigments, and diatom counts by electron microscopy.

Nutrient analyses

Total inorganic nitrogen (TIN, NO_2+NO_3+NH_4), silicate (SiO_2), and orthophosphate (PO_4) were determined. For the analysis of NO_2, NO_3, silicate, and phosphate, sub-samples of 10 mL were transferred in triplicates to 15 mL Falcon tubes and analyzed with Flow Injection autoanalyzer (Quik-Chem 8500, LACHAT Instruments). Every run was calibrated by using commercial standards with at least 5 sub-standards to cover the whole working range. For ammonium (NH_4) measurements, quadruplicates of 4 mL were transferred to 15 mL Falcon tubes and analyzed fluorometrically (Hoefer).

Chlorophyll a and phaeopigments

Triplicates of 300 mL seawater were filtered onto Whatman glass fiber filters (GF/F, 25 mm diameter, 0.7 µm pore size). The filters were incubated in 90% acetone (Carlo Erba Reagents) buffered with saturated $MgCO_3$ (Sigma-Aldrich), over-night (4 °C in darkness), and analyzed fluorometrically for chlorophyll a and phaeopigments (Brzezinski & Washburn, 2011; Jeffrey & Humphrey, 1975) (Trilogy, Turner Designs).

Electron microscopy

About 2 L of seawater were gently filtered in duplicates onto polycarbonate filters (Nuclepore Track-Etch membrane, 25 mm diameter, 0.8 µm pore size) and washed with 2mL

0.1mM NaOH to remove salt crystals (possible dissolution of diatom frustules was tested and was undetected). The filters were then dried over-night (room temperature) and coated with a thin Au/Pd film by sputter coater (Cresington 108). Representative sections of each filter were analyzed quantitatively via optical transects at two magnifications by scanning electron microscopy (Phenom Pro): x1,000 for large diatoms (> 50 µm, 100 screens per sample), and x3,000 for small diatoms (< 50 µm, 300 screens per sample). Diatoms were counted as individuals, meaning that a chain containing several cells was considered as one individual (Kenitz et al., 2020).

Data analysis

Diatom community analysis was undertaken by clustering and non-metric multidimensional scaling (NMDS). We subset the data to exclude the effect of rare species and kept only species that met two criteria: a. presence in more than 10% of all sampling points, b. contribution of at least 1% to total relative abundance in at least one sampling point. Other analyses were performed on the entire species list. Species turnover is a temporal analogue measurement of species richness, which intends to highlight the stability of the community over time, by looking on the differences of species composition between two consecutive time-points . This index was undertaken by using the R package 'codyn' (Hallett et al., 2016), measured as: $TO = \frac{S_G+S_L}{\mathrm{T}}$. Where TO is total turnover, S_G is species gained, S_L is species lost, and T is total species obsssserved in both time points. Additional data analyses were undertaken with R software, version 4.2.1 (R Core Team 2021).

Results

Temporal variation in physicochemical characteristics of the northern GoA

Diatoms were surveyed from November 2020 to June 2022, encompassing marked temporal variation in physicochemical parameters of the water column (Fig. 2). From November to

early April, SST progressively declined from >26°C to ~21°C (Fig. 2a), comprising the winter-mixing season. This temperature decline drove deep convective mixing of the water column to a maximum depth of ~400 m in April 2021 and over 700 m in April 2022. Then, from April to August the SST progressively increased and the water column became stratified. We note that the transition from the mixing to the stratified period during April occurred rapidly within less than a month, which contrasts with a much more gradual development of mixing through fall and winter (about 5 months).

The concentrations of the major macronutrients (Total inorganic nitrogen, TIN), orthophosphate (P) and silicate (Si) in surface waters (~2 m) oscillated in direct response to the seasonal mixing-stratification cycles (Fig. 2b). All macronutrients increased during the mixing season. Maximal nutrient values were concomitant with the peak of MLD in late March-early April, particularly in 2022 where mixing was deepest. In 2021, maximal concentration of TIN was 1.2 µmol L^{-1}, P was 0.09 µmol L^{-1} and Si was 0.4 µmol L^{-1}. In 2022, maximal concentrations of TIN were 2.5 µmol L^{-1}, P was 0.11 µmol L^{-1} and Si was 1.2 µmol L^{-1}. At the onset of the stratified period, TIN and P declined rapidly to lower concentrations (TIN = 0.2 and P = 0.04 µmol L^{-1} on average). A decline in Si was solely detected in 2022. During the stratified seasons, higher TIN and P were detected at the DCM as compared to the surface. The concentrations of Si during summer were comparable or higher than in winter 2021, but lower than in winter 2022.

The ratios between macronutrients highlight variations in their relative availability to phytoplankton growth (Fig. 2c). The ratio of TIN:P of 16:1 (Redfield et al., 1963) and Si:TIN of 1:1 (Brzezinski, 1985) were used as reference levels. Distinct, rapid fluctuations in TIN:P ratio between 5.8 and 22 during the mixing seasons. Peak TIN:P ratios of ~60 was detected in April 2022. During the stratified seasons, including at the DCM, TIN:P was 4.2 on average. By contrast, Si:TIN was always above 1:1 during stratified seasons (Si: TIN 3.9 on average),

but it progressively declined below 1:1 during the mixing season with minima in April (0.15 on April 7th 2022). Noticeably, Si: TIN bounced back to higher values between ~3 and >9 in May 2021 and 2022, respectively.

Phytoplankton and diatoms

Chlorophyll *a* (Chla) concentration varied in direct response to the mixing-stratified seasonal cycles as well (Fig. 2d). Peak Chla concentrations were detected in April, particularly in 2022 (2.89 µg L^{-1}) as compared to 2021 (0.51 µg L^{-1}). We defined this peak in Chla during April as the bloom. Chla during the stratified seasons was on average 0.14 µg L^{-1} at the surface and 0.36 µg L^{-1} at the DCM. At the onset of mixing in November, surface pigment levels increased on average to about 0.21 µg L^{-1} and remained approximately stable until March/April. Phaeopigments that were recorded as an indicator of predation (Shuman & Lorenzen, 1975), broadly covaried with Chla (Supplementary Fig. 1)

Total photoautotrophic cells (eukaryotes and cyanobacteria) were determined by flow cytometry (Fig 2e, Suppl. Fig. 2). Peak photosynthetic eukaryotes were detected in April during the bloom period. Peak cell concentrations were 27,469 cells mL^{-1} in April 2021 and 56,109 cells mL^{-1} in April 2022. During the stratified seasons eukaryotic concentration was on average 3,476 cells mL^{-1}. Stable concentrations were recorded until the density peak in April. Cyanobacteria concentrations peaked right after the eukaryotic bloom and declined during the mixing to minimal values around April.

Diatoms were quantified by SEM. Single cells or cell-chains were both counted as single individual (Fig. 2e). Diatom average concentrations (individuals mL^{-1}, Suppl. Fig. 3) were about 10 individuals mL^{-1} in the sea surface and about 13 individuals mL^{-1} at the DCM during the stratified season. Noticeably, during the winter-mixing period until about January, diatom concentrations remained comparable to the summer. This represented a response-

delay relative total Chla and total eukaryotic phytoplankton concentrations that incremented earlier at the onset of the mixing seasons (see above). However, around January and February a rapid increase in diatom density to about 20.7 individuals mL^{-1} was detected. This increment in diatom density coincided in both years with MLD of about 300m and an increment in TIN concentrations above 0.5 µmol L^{-1}. Maximal densities in diatoms coincided in both years with what we defined as the bloom in April. The highest yearly diatom densities of up to 393.8 ± 50.7 ind. mL-1 were detected in the 2022 bloom and 98.4 ± 11.2 ind. mL-1 in April 2021. Noticeably, the blooms of diatoms occurred at the yearly maximal nutrient concentrations and at the highest peak of TIN: P ratio (37.8 on average) but in contrast at minimal values of Si: TIN (0.31 on average). In both years, diatom maxima declined rapidly to minimal concentrations in May (12 and 6 ind. mL^{-1} in 2021 and 2022, respectively). Overall, by comparison to total eukaryotes, diatoms constituted less than 1% of the numerical photosynthetic eukaryote cell counts in most yearly time points, with the exception of the spring bloom during 2022 where diatoms reached ~6% (Suppl. Fig. 4).

Broad size-class analyses (Fig. 2f) indicated clear variations in the abundance of larger diatoms > 50 µm (which include chain-forming individuals) and smaller diatoms < 50 µm. Larger diatom accounted about 50% of total counts during most of the mixing period, but they declined in late winter such that in March prior to the blooms ~95% of the diatoms were of the smaller size class. Then, large diatom rapidly rebounded during the blooms where they accounted for ~25% of total diatoms during April 2021 and up to ~60% of total diatoms during April 2022. During the stratified seasons, large diatoms accounted for up to ~25% of total diatoms at the surface and up to ~15% of total diatoms at the DCM.

The relative contribution of centric and pennate diatoms also varied seasonally (Fig. 2f). Centric diatoms dominated from mid-winter around December/January and bloom periods, comprising from 25% to more than 90% of diatoms counts. A rapid decline in centric species

was detected after the blooms, namely following the peak event of April 2022. By contrast, during the summer month (July to October) > 95% of the diatoms were pennates.

Diatom diversity, richness and turnover

SEM analyses enabled genus or species-level taxonomic resolution for most centric diatoms, with the exception of small centric species from the family Thalassiosiraceae. In contrast, most pennate diatoms, particularly with lightly silicified frustules, could not be taxonomically identified by SEM, with the exception of *Cylindrotheca* spp. and *Pseudo-nitzschia* spp.. Henceforth, for quantitative purposes all other pennate diatoms were mostly unified in three broad size sub-categories (Large: > 50 µm; Medium: 20-50 µm; and Small: < 20µm). Representative SEM imagery of the main species is presented in Fig. 3.

A few diatoms were overall prominent in terms of concentration (Fig. 4). Among centrics, small Thalassiosiraceae (typically <10um) were the most common diatoms across seasons, but were markedly prevalent during the mixing and bloom periods reaching up to 145 individuals mL^{-1}. Large chain-forming centric species *Chaetoceros* spp. and *Leptocylindrus* spp. were also detected in most samples at average concentrations of 1.9 and 2.9 individuals mL^{-1}, respectively, but high concentrations of 39.5 and 83.7 individuals mL^{-1}, respectively, were solely detected during the densest bloom in April 2022. Few other chain forming diatom were also prominent during April 2022 such as *Rhizosolenia* spp., *Chaetoceros rostratus*, *Helicotheca sinensis*, *Lauderia annulata* and *Skeletonema grevillea* (Fig. 4). *Cylindrotheca* spp. and *Pseudo-nitzchia* spp. were the most prevalent identified pennate genera (Fig. 4) with 3.2 and 4.9 individuals mL^{-1} on average, respectively. The latter was clearly more prominent during the bloom periods reaching 84.9 individuals mL^{-1}. Otherwise, size groups of diatoms were present in most samples. Small and medium sized pennate

species (< 20 µm and 20-50 µm) were present in most samples in similar concentrations of 2.2 and 2.3 individuals mL^{-1}. Large pennates were less common (Fig. 4).

Diversity indexes, Richness and Shannon (H') were determined of the taxonomic resolution and size-class groupings obtained (Fig. 5a). Broadly, Richness and H' were higher during the mixing and bloom periods (Richness >15; H' >1.5), and rapidly declined after the bloom to minimal values in May (Richness <10; H' < 1.5). Turnover analysis was undertaken to identify period of rapid fluctuation in diatom diversity (Fig. 5b). To circumvent the overrepresentation of samples during winter, a representative sample per month was used for the analysis. The highest turnover was detected during bloom decline, particularly in 2022 (~0.9). The other time points oscillated around 0.3. A minimum turnover was detected in February 2022 at ~0.1.

Finally, Bray-Curtis similarity analysis in each sample was used to broadly outline the main diatom communities over seasons. Nine clusters of multiple samples were identified at a 65% similarity level, while five samples were too different and were left non-clustered (Fig. 6, see Suppl. Fig. 5 for details). The main species in each cluster or non-clustered sample are specified in Suppl. Table 1. The overlaying NMDS analyses enabled to link these communities to main oceanographic variables (Fig. 6). Communities X1 and X2 occurred mostly at the surface during the stratified and the early mixing periods associating with higher temperatures and low nutrients and were both largely dominated by pennate diatoms, namely *Cylindrotheca* spp. (55% of total diatoms on average), pennates smaller than 50 µm (24%), and *Pseudo-nitschia.* spp. (6%). A more dynamic succession of communities was detected later during the winter mixing seasons as nutrient availability was higher and water temperature lower. The community X3, coincided with the increase in diatom concentration

around January and comprised a more equalitarian dominance of species, including small centrics from the Thalassiosiraceae (64%) and various pennates (30%). Then communities X4, X5 and X6 rapidly succeeded during March and early-April, before the bloom peak. All these communities were dominated by small Thalassiosiraceae and pennates. The bloom periods characterized by communities X7 and X8 and were composed of Thalassiosiraceae (42%) and pennates (34%) as numerically dominant diatoms, but also members of the chain forming *Chaetoceros* as a main contributor (8%). Bloom samples associated with high TIN concentrations and high TIN:P ratios. The post-bloom samples collected in May 2022 associated with low nutrients, but high Si:TIN ratio, included community X9 and several non-clustered samples, where *Cylindrotheca* spp. was the most common diatom (30%). The samples collected in the DCM during the stratified periods were scattered in different clusters. During the early stratified periods, DCM samples were compositionally closer to late winter samples (X3, X5), while in August DCM communities resembled more surface samples from both the same period (X1) and from the early-mixing period (X2).

Spore detection and distribution

Spores from members of the chain forming *Chaetoceros* spp. were detected during the mixing and bloom periods (Fig. 7). Interannual variations in spore density were large. In 2021 spores were rare. A few spores were detected in February when diatom concentration increased during mixing, and a few more at the bloom peak in April (~3-9% of total *Chaetoceros* spp.) (Fig. 7f). However, in 2022 spore density was much higher. Spores were detected in March during the late mixing period (~4-17% of total *Chaetoceros* spp.) and then increased even further during the bloom to about 17 spores per mL, accounting for 30-50% to the density of vegetative *Chaetoceros* spp. cells (Fig, 7g). Spores were mainly detected isolated, but also within the cell chains during the bloom in 2022. In April 19th 2022, after

the bloom declined, the density of spores was much lower, but vegetative cells were completely absent and thus spores comprised 100% of *Chaetoceros* spp. individuals.

Discussion

This study details the diversity and seasonality of diatoms in the subtropical ecosystem of the GoA. Broadly, we found that diatoms form denser and more diverse assemblages, with more dynamic patterns of succession during the winter-mixing season as the input of nutrients progressively increases and the blooms that emerge at the transition between the winter mixing and stratified season. Blooms are relatively ephemeral and follow a “boom-bust” dynamics, rapidly turning-over to poorer communities within about a month. Communities detected during the stratified seasons were a lower diversity and density and appeared more stable over time. However, at the DCM communities often resembled assemblages from winter. The following sections further examine the main events detected in the GoA starting with the dynamics of the winter, bloom and finally the stratified periods and discuss its relations to diversity and ecology of diatoms in subtropical ecosystems.

Diatoms emerge late during winter-mixing

In the GoA, sea surface temperature starts declining around October, which progressively mixes up the water column, eroding the thermocline set during summer, and transports nutrients to the photic layer. This shift to turbulent environment and higher nutrient conditions triggers a transition in phytoplankton communities. Namely, *Prochlorococcus* that numerically dominates during summer, declines, while *Synechoccocus* and eukaryotic densities rapidly increase, as shown in our flow cytometry measurements and earlier studies (Al-Najjar et al., 2007; Keuter et al., 2023; Lindell & Post, 1995; Zarubin et al., 2017). Among the latter, the diversity of calcifying phytoplankton (coccolithophores) declines as

oligotrophic assemblages inhabiting the stratified layer during summer are replaced by less diverse communities dominated by r-selected species as *Gephyrocapsa huxleyi* (Keuter et al., 2023). However, by contrast, as we observed, diatoms largely did not respond to the onset of mixing, i.e., diatom density remained low and compositionally similar (as defined by NMDS with 65% similarity threshold) to the assemblages inhabiting the stratified layer during summer. Diatoms are generally categorized as r-selected organisms, capable of responding positively to nutrient inputs and to rapidly overtake phytoplankton communities in such conditions (Baillie, 1987; Margalef, 1978; McNair et al., 2018). Thus, one would expect an immediate rapid rise in diatom densities early during the mixing season. However, only later, around January/February in both surveyed years when mixing was deeper than 300 m and TIN concentration exceeded ~0.5 µmol L^{-1}, a distinct rise in diatom density and a significant shift in the compositional structure of diatom communities were detected. Incidentally, diatoms have been shown to display high minimum quota for nitrogen as compared to other phytoplankton (Litchman et al., 2007). Thus, it is plausible that at the onset of mixing in the GoA, nitrogen requirements are not met in diatoms, hampering growth relative to co-occurring smaller pico- and nanoplanktonic cells. In favor of this view, during 2022 when mixing reached greater depths earlier, the rise of the diatoms occurred a few weeks earlier than in 2021. Other abiotic parameters such as Si are critical limiting factors for diatoms in high latitude regimes (Dugdale et al., 1995; Yool & Tyrrell, 2003). However, in the GoA Si is non-limiting (Steiner et al., 2017) and lower concentrations detected later during the mixing seasons did not arrest diatom increase in density. Alternatively, specific top-down control by competition, predators or parasites could underlay their inability to respond early during the mixing season.

Shift in communities during late mixing and bloom: selective roles of nutrients and light.

Noticeably, the rise in diatom density in January/February coincided with a shift in communities, which to large extent involved an increase in numeric dominance of small centric cells with large contribution of Thalassiosiraceae (64% of diatoms). Variations in pennate diatom abundances were much less pronounced, although they still represented important fractions of the assemblages (30% of diatoms). Why specifically small centric diatoms respond to late mixing and influx of high nutrients compared to pennate cells is unclear. However, it could be that TIN limitation during early mixing is specifically applicable to centric cells as compared to pennate cells that have higher surface to volume ratios and inherently capable fulfilling nutrient uptake and requirements at lower TIN levels characteristics of summer and early mixing (see below the discussion about diatom communities from the stratified season).

Then, peaks in diatom density were detected in April concomitant with the overall Chla density peak (bloom). A much more prominent total phytoplankton and diatom bloom was detected in 2022 in correlation with a much deeper MLD and ampler nutrient densities in the photic layer. Thalassiosiraceae (42%) and pennates (34%) were the numerically dominant diatoms during bloom, but large chain forming species, namely *Chaetoceros* (8%) were also important. *Leptopcylindrus* and a few other chain forming species were also distinct, namely in 2022. Broadly, this assessment agrees with previous report in the GoA (Al-Najjar et al., 2007; Kimor & Golandsky, 1977), although here much more temporal detail was provided. It is curious to note that large chain forming species specifically flourished during the bloom period which coincided with nutrient peaks, but not before during the mixing season. Moreover, much more prominent total phytoplankton and diatom bloom were detected in 2022 in correlation with a much deeper MLD and ampler nutrient densities in the photic layer. Thus, nutrient limitation for large diatoms that have higher nutrient requirements as well as lower surface area to volume ratios (Irwin et al., 2006; Raven, 1987; Raven et al.,

2005), may hamper their development during lower conditions during earlier mixing periods and warmer winter as in 2021. In addition, light may also play an important role selecting against large chain forming species during earlier mixing periods. Prior to the bloom, deep convective mixing entrains cells through aphotic layers such that phytoplankton likely experience light limitation (Berman & Gildor, 2022). In such conditions, smaller diatom cells with higher pigment-specific absorption efficiencies could gain advantage under light limitation (Finkel, 2001; Finkel et al., 2004) and numerically dominate communities as we observed in the GoA.

Diatom bloom decay and community remodeling

From the peak of the blooms in April, diatom abundance markedly decreased towards May. This corresponds to the strongest decline in diatom diversity and highest species turnover rates detected in our survey (particularly 2022). Large-chain diatoms were mostly removed and Thalassiosiraceae declined to early mixing densities. The bloom peak coincided with Si:TIN minima and the decline to large depletion of all macronutrient pools, namely TIN, suggesting a prevalent role of nutrient limitation driving diatom bloom collapse. This assessment agrees with recent integrated model of phytoplankton blooms in the GoA (Berman & Gildor, 2022). However, additional biophysical mechanisms may be also determinant for bloom demise. For example, rapid export of large chain-diatoms and heavy diatom aggregates at the onset of stratification can be an effective mechanism to clear the photic layer of bloom biomass (Alldredge & Gotschalk, 1989; Grimm et al., 1996; Kemp et al., 2000). This could explain prevalent decline of larger species. Additionally, oceanographic models indicate that around this time period there is a strong influx of southern, warm surface water into the GoA (Biton & Gildor, 2011). These warm masses convectively spreading over the surface, deprived of Chla and nutrients, can both limit nutrients for phytoplankton growth

but also dilute local communities, leading in turn to a decrease in phytoplankton densities. Finally, a rapid drop in the Chla to phaeopigments ratio can also be detected during bloom decline. This suggests in addition that biotic factors such as grazing (Krause et al., 2010) or viruses (Kranzler et al., 2019, 2021) may be also important during bloom decline. The relative importance of bottom-up and top-down controls of diatom bloom demise requires further examination.

Emergence of diatom spores during the mixing and bloom seasons

Our study reports for the first time, the observation of diatom spores in the GoA. Spores were detected during the winter mixing and bloom in both years studied. Spores were solely assigned to members of the chain forming *Chaetoceros* group and were largely more abundant during 2022. Most of the spores appeared isolated but also within chains, indicating recent formation. The mechanisms triggering spore formation in the GoA are unclear. Particularly, spore formation in diatoms is frequently linked to adverse environmental conditions, namely nutrient limitation, decline in light intensity (Doucette & Fryxell, 1983; Smayda & Mitchell-Innes, 1974) and fluctuations in salinity (Oku & Kamatani, 1997) and/or temperature (McQuoid & Hobson, 1995). In particular, nitrogen limitation appears to be a major factor triggering diatom resting spore formation (Sugie & Kuma, 2008). Nutrient limitation is often not considered during winter in the GoA given prevalent water column mixing. However, TIN: P levels were typically erratic between time points and often below the Redfield ratio through winter and a progressive decline in the Si:TIN levels also below the Redfield ratio was also detected, both plausibly indicating nutrient limitation during the winter season. In addition, light limitation appears to affect phytoplankton populations during the mixing season, as discussed above. Thus, nutrient and/or light stress could be key triggers for sporulation in *Chaetoceros*. Furthermore, additional density-dependent cues such as

chemical signals or viral infections that can prompt spore formation in other *Chaetoceros* (Pelusi et al., 2020), could have played a key role in spore formation in the GoA, particularly in 2022 as diatom concentration was much higher. A detailed examination of the key determinant for spore formation in diatom in the GoA is required.

Finally, diatom spores serve as seed bank to subsist under sub-optimal growth conditions (Smetacek, 1985). The export and prevalence in the benthos of diatom spores were not examined in our study. However, it is likely that in the GoA, diatom spore accumulated in flanking sediments along the shoreline importantly contribute to survival rates during the oligotrophic stratified season and facilitate their re-emergence in the following winter-mixing season.

Diatoms during the stratified season

During the development of the stratified layer towards summer, nutrients become scarce in the photic layer in the GoA and a DCM appears at the base of the nutricline around 80-100m. As for most phytoplankton, diatom density was low, both in the subsurface and often even more so in the DCM. Species richness and diversity were also lower than during winter and the bloom, which contrasts with recent DNA-based studies indicating comparable in eutrophic and oligotrophic open-ocean regions (Malviya et al., 2016; Setta et al., 2023). This difference could be at least partially explained by methodological studies and ability to identify species both with molecular and microscopy-based methods, particularly in the pennate group with very low coverage in metabarcoding datasets and more difficult to identify morphologically. Clearly, both comparative analyses of both methods and additional investment on the isolation of diatoms from oligotrophic regions that can be barcoded with gene markers are important to further understand global variations in diatom diversity.

In any case, diatom community as we detected in the GoA during summer was largely comprised of small-size groups (over 91%), namely pennate species. Noticeably, pennate diatoms are typically viewed as predominantly benthic, dominating the microphytobenthos, the biofilm-forming communities that colonize intertidal and well-lit subtidal sediments (Underwood & Kromkamp, 1999), and sea-ice habitats (Poulin et al., 2011). However, as we see in the GoA and other studies have reported as well (Hulburt et al., 1960), they may be widely prevalent in the plankton and to be predominant in oligotrophic settings, where they possibly benefit characteristic higher surface to volume ratios as compare to centric diatom of equivalent size, thus gaining an advantage under nutrient limiting conditions (Raven et al., 2005), but possibly also from symbiotic associations with nitrogen-fixing cyanobacteria (Schvarcz et al., 2022), heterotrophic capabilities as it has been indicated for *Cylindrotheca* (Lewin et al., 1970) and possibly even higher thermal maxima than centric species. Examination of the eco-physiological differentiation between centric and pennate diatoms would be important to further dissect our observations and understand the prevalence of pennate cells in oligotrophic conditions.

In addition, a higher degree of resemblance between communities in the DCM during April to June and the mixing period were found and most of the main taxa detected during the mixing and bloom were detected through the summer (although at very low concentrations). These include members of *Thalassiosira*, *Cylindrotheca* and some of the main large genera found at higher densities during blooms, specifically of *Chaetoceros* and *Leptocylindrus*. Thus, the DCM may constitute a refuge for winter and bloom species for many diatom species in the GoA.

Conclusions

The pelagic realm of the GoA is typically viewed as a low productivity ecosystem that is largely dominated by single-celled cyanobacteria throughout most of the year. The diversity and importance of eukaryotes in phytoplankton assemblages has been less examined due to typical low background concentrations. However, the GoA represents a hybrid system resembling oceanic gyre system during the stratified season but it can support diatom high density spring blooms due to uniquely deep mixing dynamics and nutrient transport during winter characterized by dynamic patterns of community succession. Small-size diatom cells physiologically able to cope with low nutrient conditions during summer and possibly low light conditions during winter were numerically dominant at all seasons. However, larger diatom cells, particularly chain-forming species with high nutrient requirements, can peak during the bloom period at the onset of stratification. Mixing depth and nutrient concentration determines the extent of the bloom and the emergence of high densities of large diatom species, which was particularly visible in the second year (2022) This result highlights the critical role of the mixing layer dynamics and nutrient loads on diversity and succession patterns of diatoms at sea. Then, nutrient limitation appears to be critical for rapid bloom demise. The potential role of superimposing biotic factors regulating bloom dynamics and the importance of spores as a seed bank needs further examination. Such intense boom-bust dynamics is comparable to diatom blooms in other locations exposed to intense nutrient pulses (Alexander et al., 2015; Assmy et al., 2013; Oliver et al., 2010). Yet, diatom densities are much lower than often reported both in high latitude and coastal areas (Koeve, 2004). Following bloom termination, diatom communities remain at low background levels during oligotrophic summer both at the surface and the DCM, like it is frequently reported in gyre ecosystems (Scharek et al., 1999). Under this oligotrophic condition pennate species prevail possibly gaining advantages due to high surface to volume ratios. Clear seasonal contrasts between pennate, centric and chain forming species were overall detected, all of which

warrant further physiological assessment of the cellular mechanisms underlying such ecological differentiation. To conclude, our study provides a detailed overview of diatom diversity and ecological succession in a model subtropical ecosystem, paving the way for biogeochemical significance of diatoms in oligotrophic regions and projecting diatom responses and resilience in low latitude, warm ecosystems.

Acknowledgements

This study was supported by the Israel Science Foundation grant number 2921/20 attributed to MJF and by a PhD fellowship from the Interuniversity Institute for Marine Sciences in Eilat attributed to YA. We thank the The Israel National Monitoring Program at the Gulf of Eilat for sharing and discussing environmental data. We thank Diana Sarno and Wiebe Kooistra from Stazione Zoologica Anton Dohrn Napoli for mentoring and supporting diatom identification. We thank Tania Rivlin for inorganic nutrient measurements and Eyal Rahav, Wiebe Kooistra and Chana Kranzler for feedback comments on the study.

Conflict of interest

the authors have no conflict of interest to declare.

References

Alexander, H., Jenkins, B. D., Rynearson, T. A., & Dyhrman, S. T. (2015). Metatranscriptome analyses indicate resource partitioning between diatoms in the field. *Proceedings of the National Academy of Sciences of the United States of America*, *112*(17), E2182–E2190. https://doi.org/10.1073/pnas.1421993112

Alldredge, A. L., & Gotschalk, C. C. (1989). Direct observations of the mass flocculation of diatom blooms: characteristics, settling velocities and formation of diatom aggregates.

Deep Sea Research Part A, Oceanographic Research Papers, *36*(2), 159–171. https://doi.org/10.1016/0198-0149(89)90131-3

Al-Najjar, T., Badran, M. I., Richter, C., Meyerhoefer, M., & Sommer, U. (2007). Seasonal dynamics of phytoplankton in the Gulf of Aqaba, Red Sea. *Hydrobiologia*, *579*(1), 69–83. https://doi.org/10.1007/s10750-006-0365-z

Assmy, P., Smetacek, V., Montresor, M., Klaas, C., Henjes, J., Strass, V. H., Arrieta, J. M., Bathmann, U., Berg, G. M., Breitbarth, E., Cisewski, B., Friedrichs, L., Fuchs, N., Herndl, G. J., Jansen, S., Krägefsky, S., Latasa, M., Peeken, I., Röttgers, R., … Wolf-Gladrow, D. (2013). Thick-shelled, grazer-protected diatoms decouple ocean carbon and silicon cycles in the iron-limited Antarctic Circumpolar Current. *Proceedings of the National Academy of Sciences of the United States of America*, *110*(51), 20633–20638. https://doi.org/10.1073/pnas.1309345110

Baillie, P. W. (1987). Diatom size distributions and community stratification in estuarine intertidal sediments. *Estuarine, Coastal and Shelf Science*, *25*(2), 193–209. https://doi.org/10.1016/0272-7714(87)90122-3

Berman, H., & Gildor, H. (2022). Phytoplankton Bloom in the Gulf of Elat/Aqaba: Physical Versus Ecological Forcing. *Journal of Geophysical Research: Oceans*, *127*(5), 1–21. https://doi.org/10.1029/2021JC017922

Biton, E., & Gildor, H. (2011). Stepwise seasonal restratification and the evolution of salinity minimum in the Gulf of Aqaba (Gulf of Eilat). *Journal of Geophysical Research: Oceans*, *116*(8), 1–7. https://doi.org/10.1029/2011JC007106

Brzezinski, M. A. (1985). THE Si:C:N RATIO OF MARINE DIATOMS: INTERSPECIFIC VARIABILITY AND THE EFFECT OF SOME ENVIRONMENTAL VARIABLES.

Journal of Phycology, *21*(3), 347–357. https://doi.org/10.1111/j.0022-3646.1985.00347.x

Brzezinski, M. A., & Nelson, D. M. (1995). The annual silica cycle in the Sargasso Sea near Bermuda. *Deep Sea Research Part I: Oceanographic Research Papers*, *42*(7), 1215–1237.

Brzezinski, M. A., & Washburn, L. (2011). Phytoplankton primary productivity in the Santa Barbara Channel: Effects of wind-driven upwelling and mesoscale eddies. *Journal of Geophysical Research: Oceans*, *116*(12). https://doi.org/10.1029/2011JC007397

Buck, K. R., Chavez, F. P., & Davis, A. S. (2008). Minidiscus trioculatus, a small diatom with a large presence in the upwelling systems of central California. *Nova Hedwigia Beihefte*, *133*(1).

Busseni, G., Caputi, L., Piredda, R., Fremont, P., Hay Mele, B., Campese, L., Scalco, E., de Vargas, C., Bowler, C., d'Ovidio, F., Zingone, A., Ribera d'Alcalà, M., & Iudicone, D. (2020). Large scale patterns of marine diatom richness: Drivers and trends in a changing ocean. *Global Ecology and Biogeography*, *29*(11), 1915–1928. https://doi.org/10.1111/geb.13161

Crawford, R. M. (1995). The role of sex in the sedimentation of a marine diatom bloom. *Limnology and Oceanography*, *40*(1), 200–204. https://doi.org/10.4319/lo.1995.40.1.0200

Davis, C. O., Hollibaugh, J. T., Seibert, D. L. R., Thomas, W. H., & Harrison, P. J. (1980). Formation of Resting Spores by Leptocylindrus danicus (Bacillariophyceae) in a Controlled Experimental Ecosystem. *J. Phycol.*, *16*(2), 296–302.

Doucette, G. J., & Fryxell, G. A. (1983). Thalassiosira antarctica: vegetative and resting stage chemical composition of an ice-related marine diatom. *Marine Biology*, *78*(1), 1–6. https://doi.org/10.1007/BF00392964

Dugdale, R. C., Wilkerson, F. P., & Minas, H. J. (1995). The role of a silicate pump in driving new production. *Deep-Sea Research Part I*, *42*(5), 697–719. https://doi.org/10.1016/0967-0637(95)00015-X

Falciatore, A., & Bowler, C. (2002). Revealing the molecular secrets of marine diatoms. *Annual Review of Plant Biology*, *53*(29), 109–130. https://doi.org/10.1146/annurev.arplant.53.091701.153921

Falkowski, P. G., Barber, R. T., & Smetacek, V. (1998). Biogeochemical controls and feedbacks on ocean primary production. *Science*, *281*(5374), 200–206. https://doi.org/10.1126/science.281.5374.200

Field, C. B., Behrenfeld, M. J., Randerson, J. T., & Falkowski, P. (1998). Primary Production of the Biosphere: Integrating Terrestrial and Oceanic Components. *Science*, *281*(80), 237–240. https://doi.org/10.5194/bg-8-1477-2011

Finkel, Z. V. (2001). Light absorption and size scaling of light-limited metabolism in marine diatoms. *Limnology and Oceanography*, *46*(1), 86–94. https://doi.org/10.4319/lo.2001.46.1.0086

Finkel, Z. V., Irwin, A. J., & Schofield, O. (2004). Resource limitation alters the 3/4 size scaling of metabolic rates in phytoplankton. *Marine Ecology Progress Series*, *273*, 269–279. https://doi.org/10.3354/meps273269

Friedrichs, L., Hörnig, M., Schulze, L., Bertram, A., Jansen, S., & Hamm, C. (2013). Size and biomechanic properties of diatom frustules influence food uptake by copepods. *Marine Ecology Progress Series*, *481*(2000), 41–51. https://doi.org/10.3354/meps10227

Fryxell, G. A. (1978). CHAIN-FORMING DIATOMS: THREE SPECIES OF CHAETOCERACEAE. *Journal of Phycology*, *14*(1), 62–71. https://doi.org/10.1111/j.1529-8817.1978.tb00633.x

Genin, A., Lazar, B., & Brenner, S. (1995). Vertical mixing and coral death in the red sea following the eruption of Mount Pinatubo. *Nature*, *377*(6549), 507–510. https://doi.org/10.1038/377507a0

Grimm, K. A., Lange, C. B., & Gill, A. S. (1996). Biological forcing of hemipelagic sedimentary laminae: Evidence from ODP site 893, Santa Barbara Basin, California. In *Journal of Sedimentary Research* (Vol. 66, Issue 3, pp. 613–624). https://doi.org/10.1306/D42683C4-2B26-11D7-8648000102C1865D

Hallett, L. M., Jones, S. K., MacDonald, A. A. M., Jones, M. B., Flynn, D. F. B., Ripplinger, J., Slaughter, P., Gries, C., & Collins, S. L. (2016). codyn: An r package of community dynamics metrics. *Methods in Ecology and Evolution*, *7*(10), 1146–1151. https://doi.org/10.1111/2041-210X.12569

Hamm, C. E., Merkel, R., Springer, O., Jurkojc, P., Maiert, C., Prechtelt, K., & Smetacek, V. (2003). Architecture and material properties of diatom shells provide effective mechanical protection. *Nature*, *421*(6925), 841–843. https://doi.org/10.1038/nature01416

Hulburt, E. M., & Rodman, J. (1963). DISTRIBUTION OF PHYTOPLANKTON SPECIES WITH RESPECT TO SALINITY BETWEEN THE COAST OF SOUTHERN NEW

ENGLAND AND BERMUDA. *Limnology and Oceanography*, *8*(2), 263–269. https://doi.org/10.4319/lo.1963.8.2.0263

Hulburt, E. M., Ryther, J. H., & Guillard, R. R. L. (1960). The phytoplankton of the Sargasso Sea off Bermuda. *ICES Journal of Marine Science*, *25*(2), 115–128.

Irwin, A. J., Finkel, Z. V., Schofield, O. M. E., & Falkowski, P. G. (2006). Scaling-up from nutrient physiology to the size-structure of phytoplankton communities. *Journal of Plankton Research*, *28*(5), 459–471. https://doi.org/10.1093/plankt/fbi148

Israel National Monitoring Program NMP, www.iui-eilat.ac.il/Research/NMPAbout.aspx),. (n.d.).

Jeffrey, S. W., & Humphrey, G. F. (1975). New Spectrophotometric Equations for Determining Chlorophylls a, b, C1 and C2 in Higher Plants, Algae and Natural Phytoplankton. *Biochemie Und Physiologie Der Pflanzen*, *167*(2), 191–194.

Karl, D. M., Church, M. J., Dore, J. E., Letelier, R. M., & Mahaffey, C. (2012). Predictable and efficient carbon sequestration in the North Pacific Ocean supported by symbiotic nitrogen fixation. *Proceedings of the National Academy of Sciences of the United States of America*, *109*(6), 1842–1849. https://doi.org/10.1073/pnas.1120312109

Kemp, A. E. S., Pike, J., Pearce, R. B., & Lange, C. B. (2000). The “Fall dump” - A new perspective on the role of a “shade flora” in the annual cycle of diatom production and export flux. *Deep-Sea Research Part II: Topical Studies in Oceanography*, *47*(9–11), 2129–2154. https://doi.org/10.1016/S0967-0645(00)00019-9

Kenitz, K. M., Orenstein, E. C., Roberts, P. L. D., Franks, P. J. S., Jaffe, J. S., Carter, M. L., & Barton, A. D. (2020). Environmental drivers of population variability in colony-

forming marine diatoms. *Limnology and Oceanography*, *65*(10), 2515–2528. https://doi.org/10.1002/lno.11468

Keuter, S., Koplovitz, G., Torfstein, A., & Frada, M. J. (2023). Two-year seasonality (2017, 2018), export and long-term changes in coccolithophore communities in the subtropical ecosystem of the Gulf of Aqaba, Red Sea. *Deep-Sea Research Part I: Oceanographic Research Papers*, *191*(January 2022), 103919. https://doi.org/10.1016/j.dsr.2022.103919

Keuter, S., Young, J. R., Koplovitz, G., Zingone, A., & Frada, M. J. (2021). Novel heterococcolithophores, holococcolithophores and life cycle combinations from the families Syracosphaeraceae and Papposphaeraceae and the genus Florisphaera. *Journal of Micropalaeontology*, *40*(2), 75–99. https://doi.org/10.5194/jm-40-75-2021

Kimor, B., & Golandsky, B. (1977). Microplankton of the Gulf of Elat: Aspects of seasonal and bathymetric distribution. *Marine Biology*, *42*(1), 55–67. https://doi.org/10.1007/BF00392014

Koeve, W. (2004). Spring bloom carbon to nitrogen ratio of net community production in the temperate N. Atlantic. *Deep-Sea Research Part I: Oceanographic Research Papers*, *51*(11), 1579–1600. https://doi.org/10.1016/j.dsr.2004.07.002

Kranzler, C. F., Brzezinski, M. A., Cohen, N. R., Lampe, R. H., Maniscalco, M., Till, C. P., Mack, J., Latham, J. R., Bruland, K. W., Twining, B. S., Marchetti, A., & Thamatrakoln, K. (2021). Impaired viral infection and reduced mortality of diatoms in iron-limited oceanic regions. *Nature Geoscience*, *14*(4), 231–237. https://doi.org/10.1038/s41561-021-00711-6

Kranzler, C. F., Krause, J. W., Brzezinski, M. A., Edwards, B. R., Biggs, W. P., Maniscalco, M., McCrow, J. P., Van Mooy, B. A. S., Bidle, K. D., Allen, A. E., & Thamatrakoln, K.

(2019). Silicon limitation facilitates virus infection and mortality of marine diatoms. *Nature Microbiology*, *4*(11), 1790–1797. https://doi.org/10.1038/s41564-019-0502-x

Krause, J. W., Brzezinski, M. A., Landry, M. R., Baines, S. B., Nelson, D. M., Selph, K. E., Taylor, A. G., & Twining, B. S. (2010). The effects of biogenic silica detritus, zooplankton grazing, and diatom size structure on silicon cycling in the euphotic zone of the eastern equatorial Pacific. *Limnol. Oceanogr*, *55*(6), 2608–2622. https://doi.org/10.4319/lo2010.55.6.2608

Kuwata, A., Hama, T., & Takahashi, M. (1993). Ecophysiological characterization of two life forms, resting spores and resting cells, of a marine planktonic diatom, Chaetoceros pseudocurvisetus , formed under nutrient depletion. *Mar. Ecol. Prog. Ser*, *102*, 245–255.

Lassiter, A. M., Wilkerson, F. P., Dugdale, R. C., & Hogue, V. E. (2006). Phytoplankton assemblages in the CoOP-WEST coastal upwelling area. *Deep-Sea Research Part II: Topical Studies in Oceanography*, *53*(25–26), 3063–3077. https://doi.org/10.1016/j.dsr2.2006.07.013

Leblanc, K., Quéguiner, B., Diaz, F., Cornet, V., Michel-Rodriguez, M., Durrieu De Madron, X., Bowler, C., Malviya, S., Thyssen, M., Grégori, G., Rembauville, M., Grosso, O., Poulain, J., De Vargas, C., Pujo-Pay, M., & Conan, P. (2018). Nanoplanktonic diatoms are globally overlooked but play a role in spring blooms and carbon export. *Nature Communications*, *9*(1), 1–12. https://doi.org/10.1038/s41467-018-03376-9

Lewin, J., Hellebust, J. A., & Lewin, J. (1970). Heterotrophic nutrition of the marine pennate diatom, Cylindrotheca fusiformis. *Canadian Journal of Microbiology*, *16*(11), 1123–1129.

Lindell, D., & Post, A. F. (1995). Ultraphytoplankton succession is triggered by deep winter mixing in the Gulf of Aqaba (Eilat), Red Sea. *Limnology and Oceanography*, *40*(6), 1130–1141. https://doi.org/10.4319/lo.1995.40.6.1130

Litchman, E., Klausmeier, C. A., Schofield, O. M., & Falkowski, P. G. (2007). The role of functional traits and trade-offs in structuring phytoplankton communities: Scaling from cellular to ecosystem level. *Ecology Letters*, *10*(12), 1170–1181. https://doi.org/10.1111/j.1461-0248.2007.01117.x

López-Sandoval, D. C., Rodríguez-Ramos, T., Cermeño, P., Sobrino, C., & Marañón, E. (2014). Photosynthesis and respiration in marine phytoplankton: Relationship with cell size, taxonomic affiliation, and growth phase. *Journal of Experimental Marine Biology and Ecology*, *457*, 151–159. https://doi.org/10.1016/j.jembe.2014.04.013

Malviya, S., Scalco, E., Audic, S., Vincent, F., Veluchamy, A., & Poulain, J. (2016). *Insights into global diatom distribution and diversity in the world ' s ocean*. https://doi.org/10.1073/pnas.1509523113

Margalef, R. (1978). Life-forms of phytoplankton as survival alternatives in an unstable environment. *Oceanol. Acta*, *1*(4), 493–509. https://doi.org/10.1007/BF00202661

McNair, H. M., Brzezinski, M. A., & Krause, J. W. (2018). Diatom populations in an upwelling environment decrease silica content to avoid growth limitation. *Environmental Microbiology*, *20*(11), 4184–4193. https://doi.org/10.1111/1462-2920.14431

McQuoid, M. R., & Hobson, L. A. (1995). Importance of Resting Stages in Diatom Seasonal Succession. *Journal of Phycology*, *31*(1), 44–50. https://doi.org/10.1111/j.0022-3646.1995.00044.x

Nelson, D. M., Tréguer, P., Brzezinski, M. A., Leynaert, A., & Quéguiner, B. (1995). Production and dissolution of biogenic silica in the ocean: Revised global estimates, comparison with regional data and relationship to biogenic sedimentation. *Global Biogeochemical Cycles*, *9*(3), 359–372. https://doi.org/10.1029/95GB01070

Oku, O., & Kamatani, A. (1995). Resting spore formation and phosphorus composition of the marine diatom Chaetoceros pseudocurvisetus under various nutrient conditions. *Marine Biology*, *123*(2), 393–399. https://doi.org/10.1007/BF00353630

Oku, O., & Kamatani, A. (1997). Resting spore formation of the marine planktonic diatom Chaetoceros anastomosans induced by high salinity and nitrogen depletion. *Marine Biology*, *127*(3), 515–520. https://doi.org/10.1007/s002270050040

Oliver, M. J., Schofield, O., & Bidle, K. (2010). Density dependent expression of a diatom retrotransposon. *Marine Genomics*, *3*(3–4), 145–150. https://doi.org/10.1016/j.margen.2010.08.006

Pelusi, A., De Luca, P., Manfellotto, F., Thamatrakoln, K., Bidle, K. D., & Montresor, M. (2021). Virus-induced spore formation as a defense mechanism in marine diatoms. *New Phytologist*, *229*(4), 2251–2259. https://doi.org/10.1111/nph.16951

Pelusi, A., Margiotta, F., Passarelli, A., Ferrante, M. I., Ribera d'Alcalà, M., & Montresor, M. (2020). Density-dependent mechanisms regulate spore formation in the diatom Chaetoceros socialis. *Limnology And Oceanography Letters*, *5*(5), 371–378. https://doi.org/10.1002/lol2.10159

Polovina, J. J., Howell, E. A., & Abecassis, M. (2008). Ocean's least productive waters are expanding. *Geophysical Research Letters*, *35*(3). https://doi.org/10.1029/2007GL031745

Poulin, M., Daugbjerg, N., Gradinger, R., Ilyash, L., Ratkova, T., & von Quillfeldt, C. (2011). The pan-Arctic biodiversity of marine pelagic and sea-ice unicellular eukaryotes: A first-attempt assessment. In *Marine Biodiversity* (Vol. 41, Issue 1, pp. 13–28). https://doi.org/10.1007/s12526-010-0058-8

R Core Team (2021). R: A language and environment for statistical computing. R Foundation for Statistical Computing (4.2.1). (n.d.). https://www.r-project.org/

Raven, J. A. (1987). The Role of Vacuoles. *New Phytologist*, *106*(3), 357–422.

Raven, J. A., Finkel, Z. V., & Irwin, A. J. (2005). Picophytoplankton: bottom-up and top-down controls on ecology and evolution. *Vie et Milieu/Life & Environment*, 209–215.

Redfield, A. C., Ketchum, B. H., & Richards, F. A. (1963). The influence of organisms on the composition of seawater. In *The sea* (Vol. 2, pp. 26–77).

Riebesell, U. (2000). Carbon fix for a diatom. *Nature*, *407*(6807), 959–960.

Rogato, A., Amato, A., Iudicone, D., Chiurazzi, M., Ferrante, M. I., & d'Alcalà, M. R. (2015). The diatom molecular toolkit to handle nitrogen uptake. *Marine Genomics*, *24*, 95–108. https://doi.org/10.1016/j.margen.2015.05.018

Round, F. E. (1981). Some aspects of the origin of diatoms and their subsequent evolution. *BioSystems*, *14*, 483–486.

Round, F. E., Crawford, R. M., & Mann, D. G. (1990). *Diatoms: biology and morphology of the genera*.

Ruggiero, M. V., D'Alelio, D., Ferrante, M. I., Santoro, M., Vitale, L., Procaccini, G., & Montresor, M. (2018). Clonal expansion behind a marine diatom bloom. *ISME Journal*, *12*(2), 463–472. https://doi.org/10.1038/ismej.2017.181

Sarthou, G., Timmermans, K. R., Blain, S., & Tréguer, P. (2005). Growth physiology and fate of diatoms in the ocean: A review. *Journal of Sea Research*, *53*(1-2 SPEC. ISS.), 25–42. https://doi.org/10.1016/j.seares.2004.01.007

Savidge, G., Boyd, P., Pomroy, A., Harbour, D., & Joint, I. (1995). Phytoplankton production and biomass estimates in the northeast Atlantic Ocean, May-June 1990. *Deep-Sea Research Part I*, *42*(5), 599–617. https://doi.org/10.1016/0967-0637(95)00016-Y

Scharek, R., Latasa, M., Karl, D. M., & Bidigare, R. R. (1999). Temporal variations in diatom abundance and downward vertical flux in the oligotrophic North Pacific gyre. *Deep Sea Research Part I: Oceanographic Research Papers*, *46*(6), 1051–1075.

Schvarcz, C. R., Wilson, S. T., Caffin, M., Stancheva, R., Li, Q., Turk-Kubo, K. A., White, A. E., Karl, D. M., Zehr, J. P., & Steward, G. F. (2022). Overlooked and widespread pennate diatom-diazotroph symbioses in the sea. *Nature Communications*, *13*(1). https://doi.org/10.1038/s41467-022-28065-6

Setta, S. P., Lerch, S., Jenkins, B. D., Dyhrman, S. T., & Rynearson, T. A. (2023). Oligotrophic waters of the Northwest Atlantic support taxonomically diverse diatom communities that are distinct from coastal waters. *Journal of Phycology*, *59*(6), 1202–1216. https://doi.org/10.1111/jpy.13388

Shuman, R., & Lorenzen, C. J. (1975). Quantitative degradation of chlorophyll by a marine herbivore. *Limnology and Oceanography*, *20*(4), 580–586.

Smayda, T. J., & Mitchell-Innes, B. (1974). Dark survival of autotrophic, planktonic marine diatoms. *Marine Biology*, *25*(3), 195–202. https://doi.org/10.1007/BF00394965

Smetacek, V. S. (1985). Role of sinking in diatom life-history cycles: ecological, evolutionary and geological significance. *Marine Biology*, *84*(3), 239–251. https://doi.org/10.1007/BF00392493

Steiner, Z., Lazar, B., Torfstein, A., & Erez, J. (2017). Testing the utility of geochemical proxies for paleoproductivity in oxic sedimentary marine settings of the Gulf of Aqaba, Red Sea. *Chemical Geology*, *473*(March), 40–49. https://doi.org/10.1016/j.chemgeo.2017.10.012

Sugie, K., & Kuma, K. (2008). Resting spore formation in the marine diatom Thalassiosira nordenskioeldii under iron- and nitrogen-limited conditions. *Journal of Plankton Research*, *30*(11), 1245–1255. https://doi.org/10.1093/plankt/fbn080

Tréguer, P., Bowler, C., Moriceau, B., Dutkiewicz, S., Gehlen, M., Aumont, O., Bittner, L., Dugdale, R., Finkel, Z., Iudicone, D., Jahn, O., Guidi, L., Lasbleiz, M., Leblanc, K., Levy, M., & Pondaven, P. (2018). Influence of diatom diversity on the ocean biological carbon pump. In *Nature Geoscience* (Vol. 11, Issue 1, pp. 27–37). Nature Publishing Group. https://doi.org/10.1038/s41561-017-0028-x

Tréguer, P., Nelson, D. M., Van Bennekom, A. J., Demaster, D. J., Leynaert, A., & Quéguiner, B. (1995). The silica balance in the world ocean: A reestimate. *Science*, *268*(5209), 375–379. https://doi.org/10.1126/science.268.5209.375

Underwood, G. J. C., & Kromkamp, J. (1999). Primary production by phytoplankton and microphytobenthos in estuaries. In *Estuaries* (pp. 93–153).

Yool, A., & Tyrrell, T. (2003). Role of diatoms in regulating the ocean's silicon cycle. *Global Biogeochemical Cycles*, *17*(4). https://doi.org/10.1029/2002gb002018

Zarubin, M., Lindemann, Y., & Genin, A. (2017). The dispersion-confinement mechanism: Phytoplankton dynamics and the spring bloom in a deeply-mixing subtropical sea. *Progress in Oceanography*, *155*, 13–27. https://doi.org/10.1016/j.pocean.2017.05.005

Figures

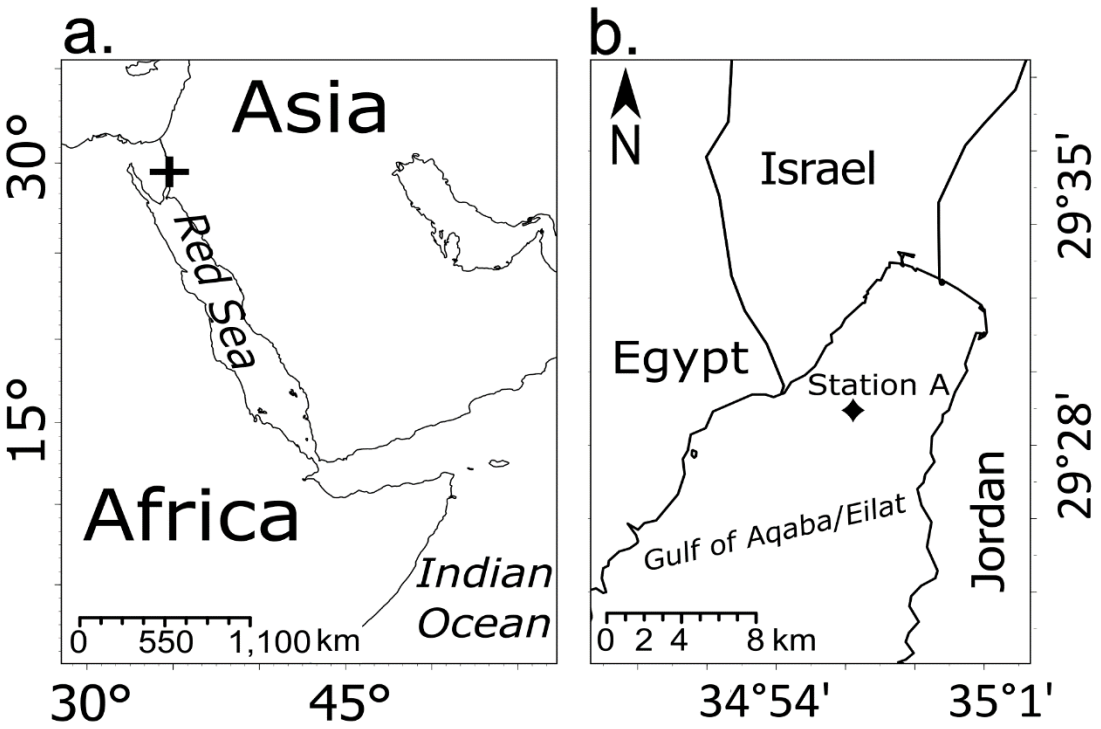

Figure 1. Map of the (a) Red Sea and (b) Gulf of Aqaba (GoA). The Red Sea, connected to the Indian Ocean and the GoA, the northeaster tip of the Red Sea, indicated as plus in a. The 'Station A', the open sea sampling station in this study is indicated as filled square in b.

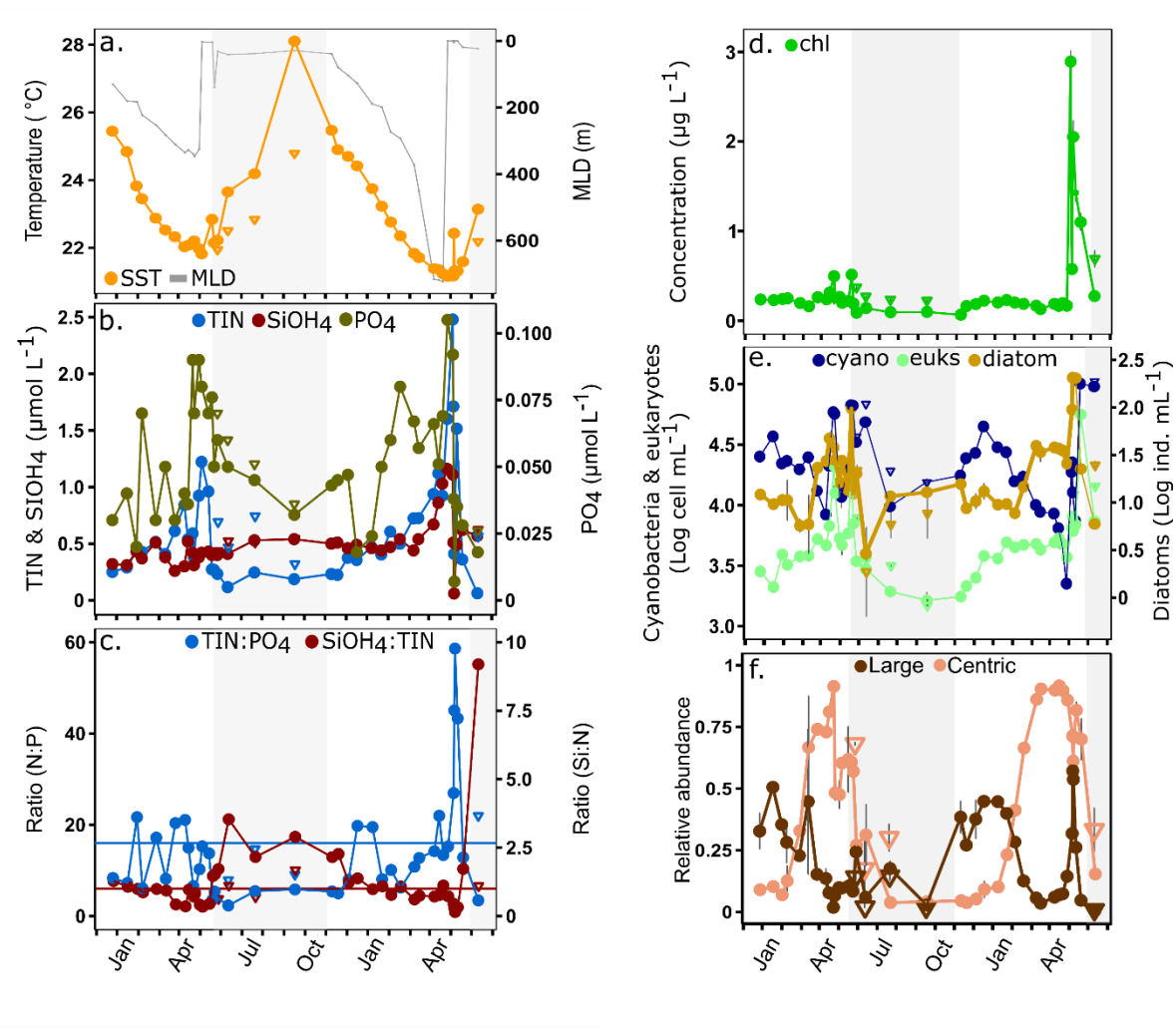

Figure 2. Seasonal dynamics of environmental variables, algal pigments, and algal abundances in the Gulf of Aqaba. The shaded grey area represents the stratified season. Measurements undertaken during the stratified seasons at the DCM are presented in triangle symbols. (a) Temperature (sea surface temperature (SST) and DCM) and the mixed layer depth (MLD). (b) Macronutrients: total inorganic nitrogen (TIN), silicon, and phosphate. (c) Ratios of main macronutrients in the sub-surface: TIN: P and Si: TIN. The horizontal lines represent of Redfield ratio for TIN: P (16:1, blue), and Si: TIN (1:1, red). (d) Chlorophyll a density. Grey bars represent standard deviation (n=3). (e) Averaged log-transformed concentration of total eukaryotic phytoplankton, total cyanobacteria (*Prochlorococcus* and *Synechococcus*) and diatom densities. Grey bars represent standard deviation (n = 2). Data of cyanobacteria and eukaryotes is based on flow cytometry counts, diatoms were counted by scanning electron microscopy. (f) Relative abundance of large diatoms (> 50 µm, compared to smaller diatoms, brown) and of centric diatoms (compared to pennate, pink). Grey bars represent standard deviation (n=2).

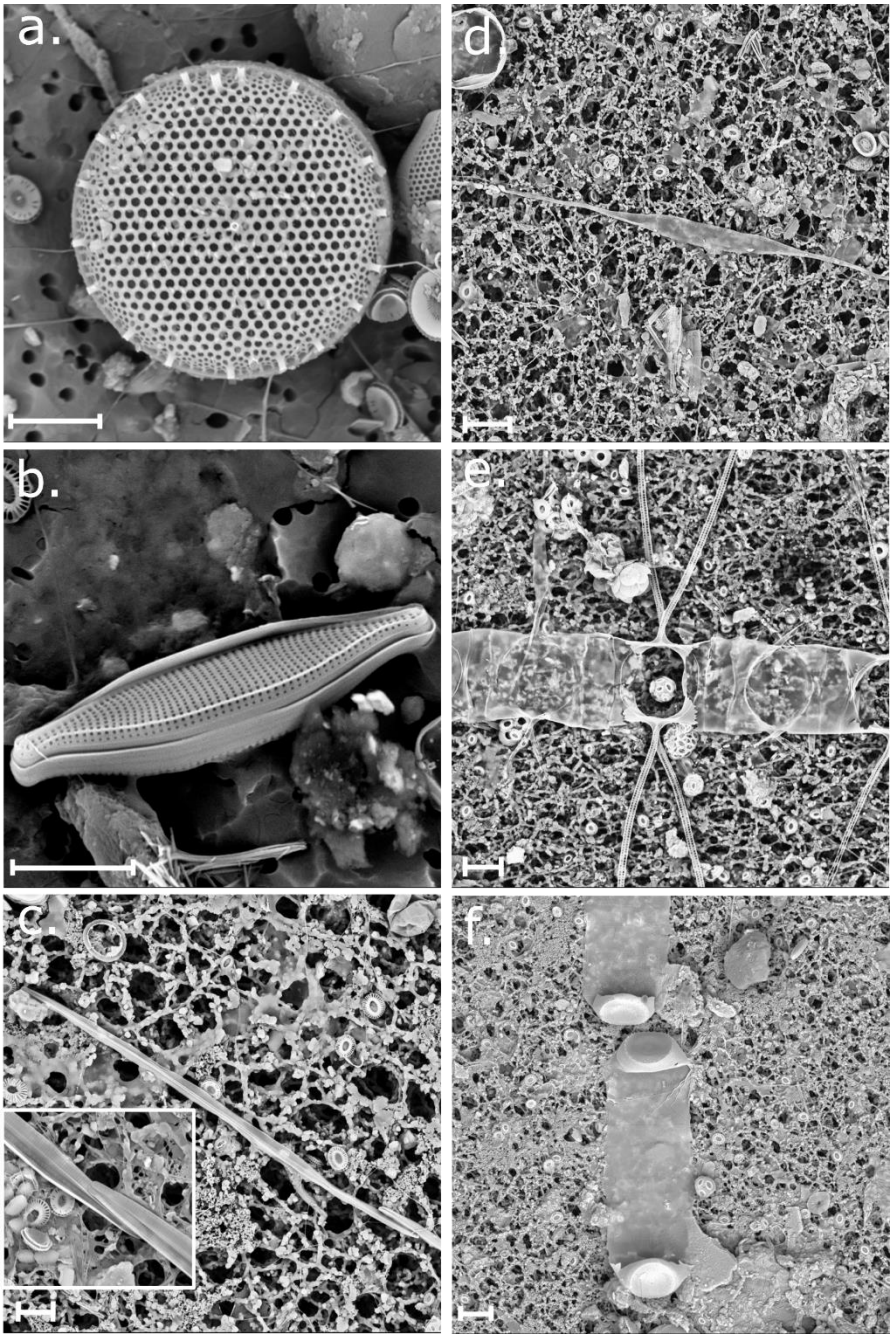

Figure 3. Main diatom species in the GoA. (a) centric diatom from Thalassiosiraceae family; key contributor to the small size-fraction. (b) An unidentified pennate. This group was classified into 3 size-based groups (both in the small and large size-fractions). (c) Chain of the pennate *Pseudo-nitzschia* spp., attachment of valves is shown in inset. (d) A pennate *Cylindrotheca* spp., which appeared in both small and large size fractions. (e) Chain-forming centric *Chaetoceros*; notable representative of the large size-fraction during the bloom. (f) A chain-forming centric *Leptocylindrus*. Scale = 5 µm (a-c), 10 µm (d-f).

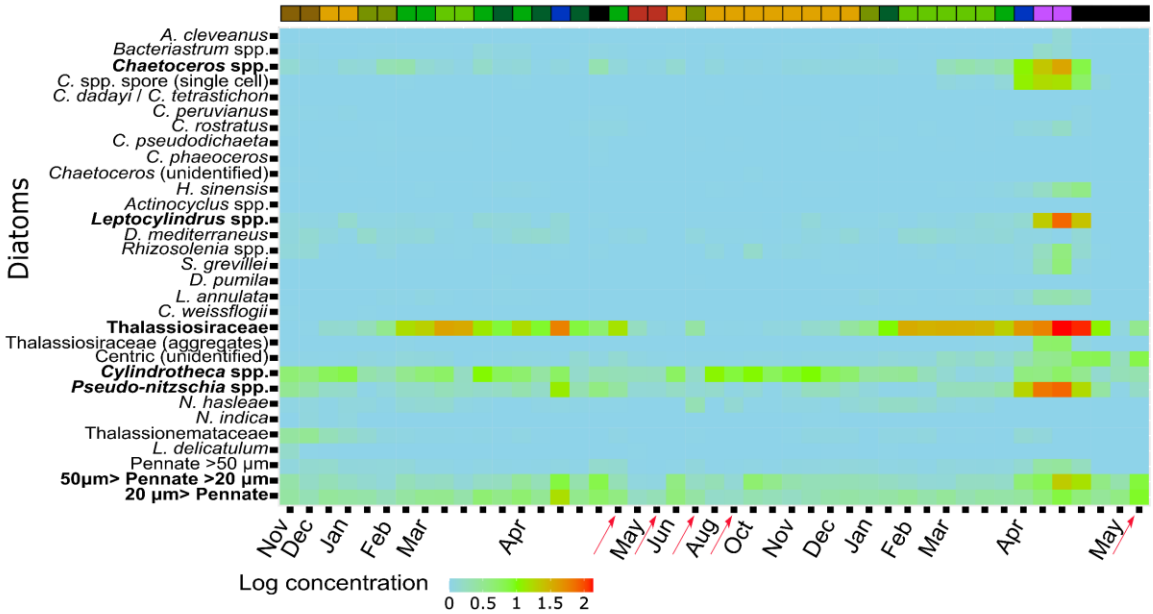

Figure 4. Heatmap of diatom groups composition between 2020-2022. Blue-white gradient represents log-transformed concentrations (electron microscopy counts). The red arrows represent DCM samples. The color code on top of the heatmap refers to the diatom community cluster, based on 65% similarity (Bray-Curtis index. For further information see Suppl. Fig. 5).

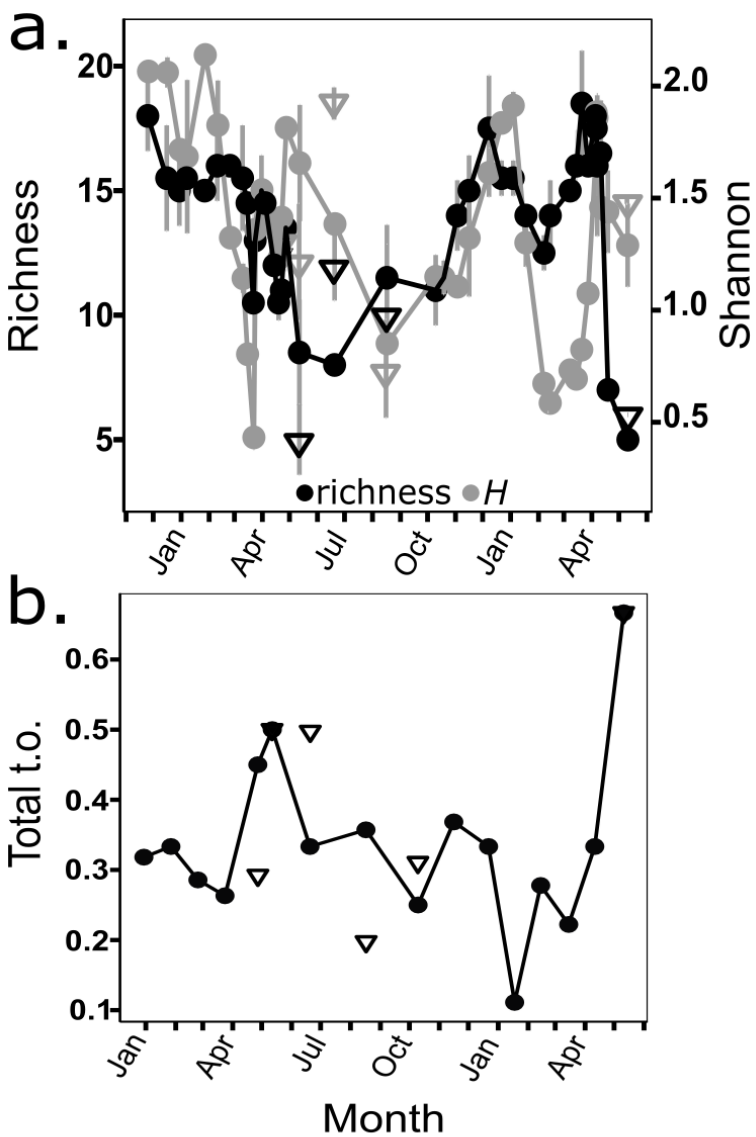

Figure 5. Diatom diversity indices. Circles connected with line represent 2m depth, while triangles represent samples from the deep chlorophyll maximum (DCM). (a) Diatom species richness (black) and Shannon index (grey). Grey bars represent standard deviation (n=2). (b) Diatom species turnover index. This index detects differences between time points in appearance and disappearance of diatom taxa.

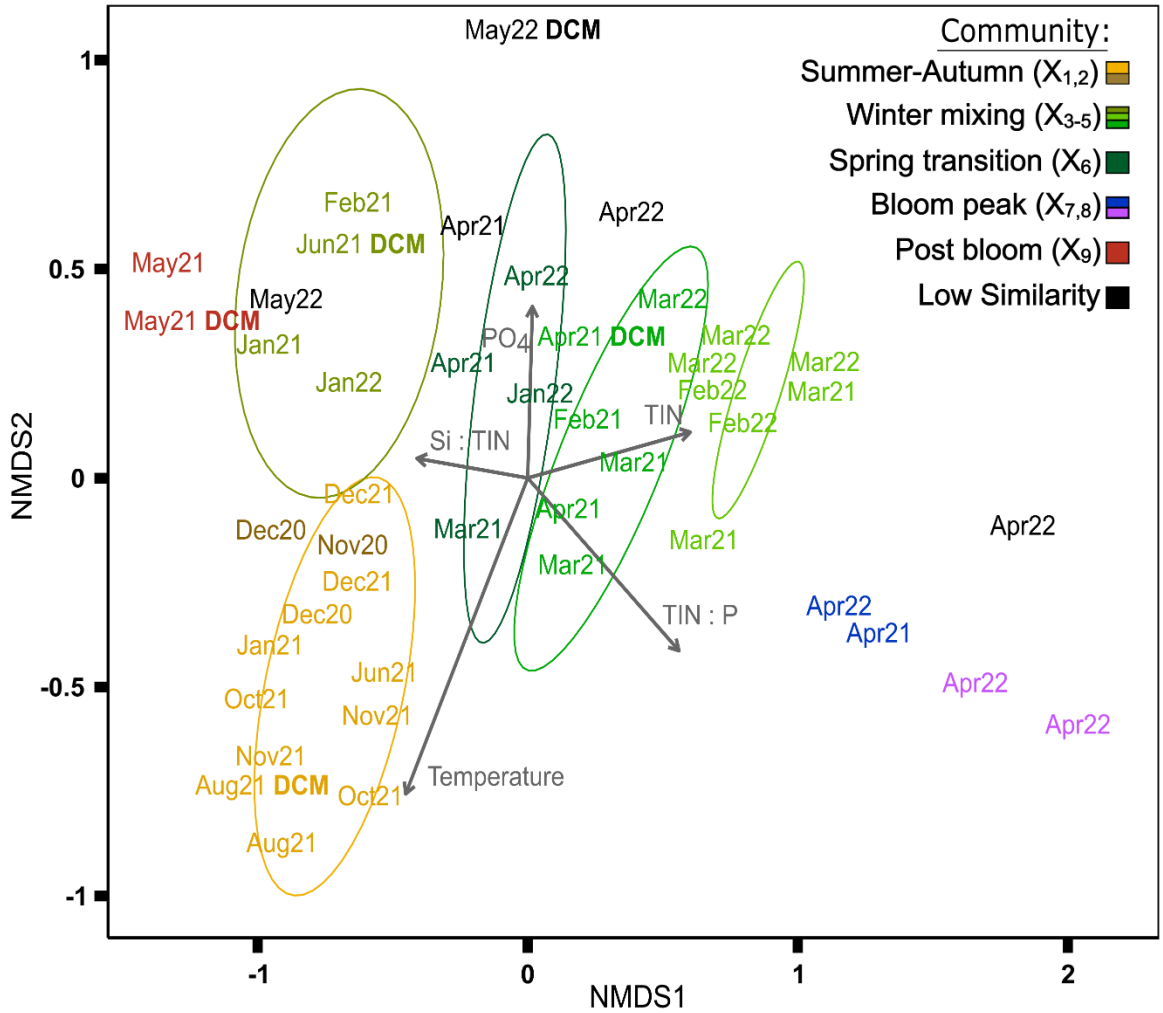

Figure 6. NMDS ordination of diatom communities (Bray-Curtis distance). The color code shows communities with ≥ 65% similarity and represent clusters: Orange, brown: summer and autumn. Light green (3 sub-clusters): winter mixing. Dark green: transition from mixing to stratification. Blue, pink: spring bloom. Red: post bloom. Black shows communities with < 65% similarity to other samples. Grey arrows represent significant environmental variables ($p < 0.05$).

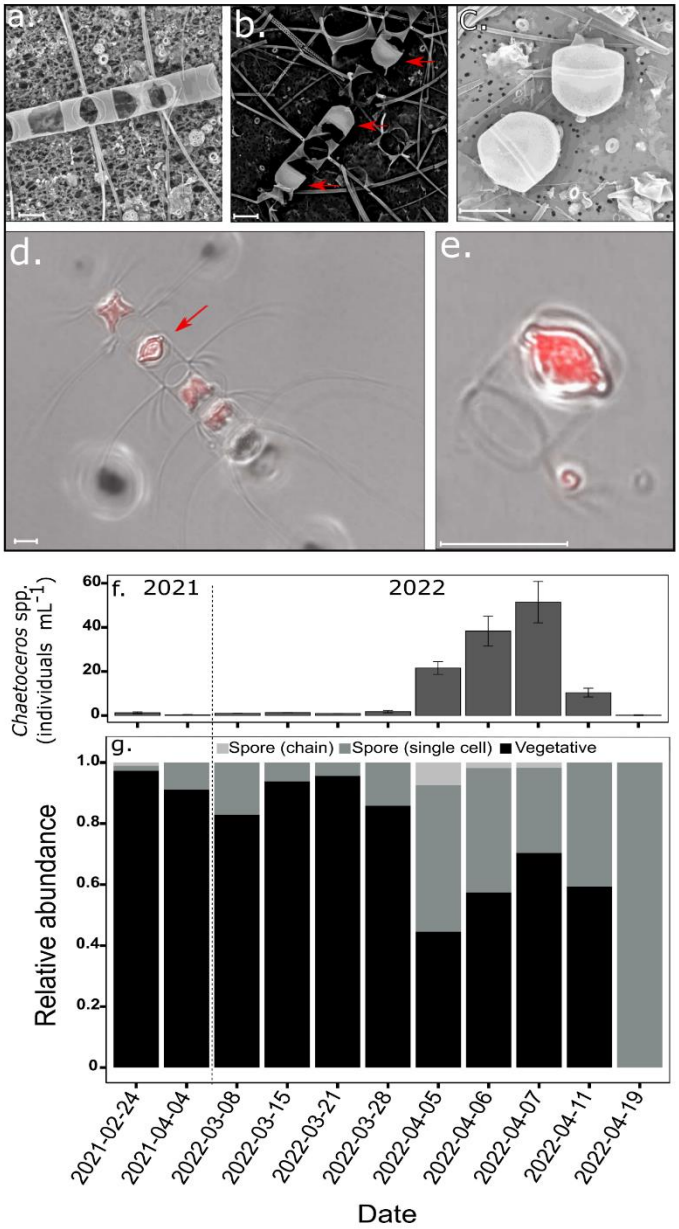

Figure 7. Life-stages of *Chaetoceros* spp. via scanning electron microscopy (a-c) and light-microscopy (d,e). (a) Chain of vegetative cells. (b) A chain, including spores (red arrows) and a vegetative cell. (c) Spores as single cells. (d) A chain, including a spore (red arrow) and vegetative cells. (e) Spore as a single cell. Two layers are presented in light-microscopy: Brightfield (grey) for cell morphology, and chlorophyll autofluorescence (red, EX:649 nm/EM:670 nm). Scale: 10 µm. (f) Concentration of total *Chaetoceros* spp. individuals (including vegetative and spore life forms) by SEM counts. Bars represent standard deviation (n=2). (g) Relative abundance (between 0-1) of vegetative cells and spores of the chain forming *Chaetoceros* spp. species complex, in samples where spores were detected. Black= vegetative cells, grey= spores found as a single cell, light-grey= spores found in a chain.